Nanoscale

COMMUNICATION

View Article Online
View Journal | View Issue

Graphene-induced unusual microstructural evolution in Ag plated Cu foils†

Cite this: *Nanoscale*, 2014, **6**, 7209

Hae-A-Seul Shin,[a] Jaechul Ryu,[bc] Seungmin Cho,[c] Byung Hee Hong*[b] and Young-Chang Joo*[ad]

Received 3rd March 2014
Accepted 25th April 2014

DOI: 10.1039/c4nr01163e

www.rsc.org/nanoscale

Graphene-induced abnormal grain growth of Cu with a grain size of more than 1 mm^2 was observed on Cu–Ag alloy foil, and this phenomenon occurred only with graphene synthesis and only on the Cu–Ag alloy among various types of Cu foils.

Graphene, a one-atom-thick film composed of carbon atoms arranged in a regular hexagonal pattern, has received much attention from many researchers due to its fascinating electrical, mechanical, optical, and thermal properties.[1–6] The well-controlled synthesis of graphene, one of the key enablers for the successful application of graphene in various research areas, remains the most important issue in its research. For the synthesis of a highly uniform and large sized graphene film with few defects, many researchers are interested in the effects of Cu microstructures, such as grain boundaries, Cu orientation and defects in Cu.[7–9] Therefore, previous studies on the interactions between graphene and the Cu catalytic substrate have focused only on the effects of Cu on graphene synthesis and quality of synthesized graphene. However, graphene synthesized on Cu may also have some effects on the Cu microstructure, as we demonstrate in this manuscript; until now, few studies have focused on the effects of graphene on Cu or other metal catalysts. There is a report of periodic surface depression on Cu induced by graphene;[10] however, these patterns were only generated by a post-annealing process after graphene synthesis.

In this study, we first report an unusual microstructural evolution of Cu with graphene synthesis. Abnormal grain growth of Cu, which was more than the mm^2 scale of giant grain size, was observed for the dilute Cu–Ag alloy catalyst with graphene synthesis, in contrast to the μm^2 scale of grain size for conventional Cu foil. The Cu–Ag alloy is an advanced material for a catalyst of graphene synthesis, as we reported in our previous paper,[11] and the unusual microstructural evolution of Cu was observed only for this Cu–Ag alloy catalyst. In addition, the abnormal grain growth was developed with the evolution of a uniform cube texture. Generally, the cube texture is observed in heavily rolled and/or high purity Cu for rolled Cu foil,[12,13] so the addition of Ag for alloying may have reduced the development of the cube texture in this study. However, large areas of cube texture were developed in Cu with graphene synthesis on our dilute Cu–Ag alloy catalyst.

Abnormal grain growth has been found in metal thin films with deposition and post-annealing processes.[14–16] The grain size distribution and texture depend on the relative magnitude of stresses, such as surface energy or strain energy between grains, which can be induced by the substrate, deposition parameters and annealing conditions with various film thicknesses.[14] Our results suggest that graphene could also influence the stress on Cu and that graphene formation on Cu is a driving force for abnormal grain growth of Cu. The effects of graphene and substitutional Ag in Cu will be discussed in detail in this manuscript.

Two types of Cu foil were prepared to compare their microstructure after graphene synthesis: 35 μm thick Cu foil (purity 99.85%, Japan Energy Co.) without surface plating and Cu foil with 200 nm thick Ag plating. Ag was electroplated using potassium silver cyanide as an electrolyte with a deposition rate of 5.0 μm min^{-1} at a current density of 10 ASD (ampere per square decimeter).

Then, graphene was synthesized using a thermal chemical vapor deposition (CVD) system with a 4-inch quartz tube (Graphene Square Inc.). Each catalytic substrate (5 × 7 cm^2 in size) was inserted inside the quartz tube and then heated from room temperature to the synthesis temperatures of 900 °C or 1000 °C. The temperature of the CVD chamber was ramped up at a rate of

[a]*Department of Materials Science & Engineering, Seoul National University, Seoul 151-744, Republic of Korea. E-mail: ycjoo@snu.ac.kr*

[b]*Department of Chemistry, Seoul National University, Seoul 151-747, Republic of Korea. E-mail: byunghee@snu.ac.kr*

[c]*Samsung Techwin Co., Ltd., Seongnam 463-400, Republic of Korea*

[d]*Research Institute of Advanced Materials (RIAM), Seoul National University, Seoul 151-742, Korea*

† Electronic supplementary information (ESI) available: A detailed texture analysis of Cu EBSD orientation maps and grain size calculation. See DOI: 10.1039/c4nr01163e

20 °C min^{-1} with flowing 8 sccm of H_2. After reaching the target synthesis temperatures, CH_4 gas was injected with a flow rate of 35 sccm, and the H_2 flow was maintained with 8 sccm at 1000 mTorr for 40 min. For the annealing of Cu and Cu–Ag, the temperature profile and H_2 gas flow were the same except for the injection of CH_4 gas at the annealing temperatures (900 °C or 1000 °C). Finally, the CVD furnace was moved from the sample to fast-cooling and the sample was quenched to room temperature with flowing H_2 at 70 mTorr after graphene synthesis and annealing.

Ag plated Cu formed a dilute Cu–Ag alloy (maximum 0.79 at% of Ag in Cu) with graphene synthesis, as demonstrated in our previous report.[11] The textures of the Cu foil and the Cu–Ag alloy were carefully characterized by electron backscatter diffraction (EBSD), and the graphene morphology and the Cu surface were observed by scanning electron microscopy (SEM, Hitachi SU-70) and energy dispersive spectrometry (EDS).

Fig. 1a–d show the EBSD orientation maps of Cu and Cu–Ag with graphene (after graphene synthesis at 900 °C or 1000 °C with CH_4 gas for 40 min) and without graphene (after annealing at 900 °C or 1000 °C for 40 min). The EBSD orientation maps in Fig. 1a–d are the results from the normal direction (ND; the vertical direction for the surface of graphene-synthesized Cu), and for consideration of the orientation maps from all directions, the Cu texture was mostly (100)⟨100⟩, *i.e.*, cube texture.[12,13] Texture analysis with the rolling direction (RD) and the transverse direction (TD) also showed (100) orientation. The EBSD data of the cube texture are discussed in the ESI.†

The average grain size of Cu and the ratio of the (100) texture are compared in Fig. 1e and f. The ratio of the cube texture for Cu with graphene synthesis was 54.9% at 900 °C and 59.1% at 1000 °C, respectively. However, the ratio of the cube texture for Cu–Ag with graphene synthesis was 92.7% and 98.1% at 900 °C and 1000 °C, respectively. Although the (100) texture was the dominant texture for both Cu and Cu–Ag with graphene syntheses, the ratio of (100) of Cu–Ag with graphene synthesis was significantly larger than that of Cu. The ratio of (100) was more than 90%, and most of the orientation of Cu–Ag was

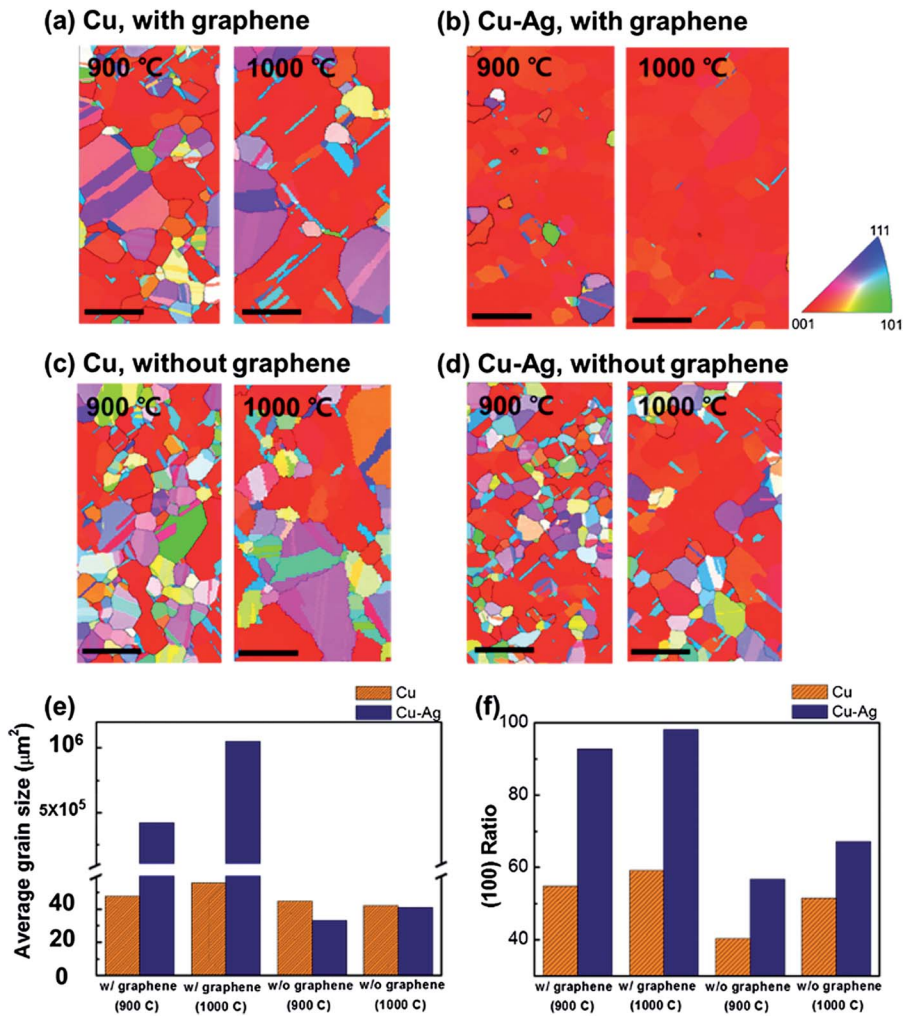

Fig. 1 EBSD orientation maps of Cu with graphene synthesis on (a) Cu and (b) Cu–Ag and without graphene on (c) Cu and (d) Cu–Ag at 900 °C, 1000 °C for 40 min; scale bars (200 μm). (e) The average grain size of Cu and (f) the ratio of the (100) texture with graphene synthesis and without graphene on Cu and Cu–Ag at 900 °C and 1000 °C.

changed to the cube texture with graphene synthesis. This orientation change to one texture induced the abnormal grain growth of Cu, which only occurred in the case of Cu–Ag with graphene synthesis. Although the average grain size in Cu foil with graphene synthesis at 1000 °C was 56 μm^2, that in Cu–Ag with graphene synthesis at 1000 °C was over 1.05 mm^2, which was 18 750 times larger than the average grain size in the Cu foil with graphene. Grain boundary analysis was conducted with the criteria of 5° misorientation angle. The detailed analysis process of the grain size calculation is explained in the ESI.† The grain size of Cu–Ag was the maximized measurement area of EBSD at one time (*i.e.*, it reached the upper limit of measurable area of the EBSD instrument used in this study), and the Cu–Ag formed almost one single grain within this area.

There is a possibility that the microstructural evolution of Cu–Ag was just caused by the formation of the Cu–Ag alloy (irrespective of the graphene synthesis on Cu). To demonstrate the effects of Cu–Ag alloy formation exclusive of graphene synthesis, the Cu texture in Cu foil and Cu–Ag was analyzed after annealing (without graphene synthesis) at 900 °C and 1000 °C. Fig. 1c and d show the EBSD orientation maps of Cu and Cu–Ag without graphene at 900 °C and 1000 °C for 40 min. The ratios of (100) in Cu without graphene (annealing at 900 °C and 1000 °C) were 40.4% and 51.6%, respectively, and the ratios of (100) in Cu–Ag without graphene were 56.7% and 67.2%, respectively. In contrast to the results from the graphene synthesis, the (100) texture in Cu–Ag without graphene was relatively small. The ratio of (100) in Cu–Ag without graphene was higher than that in Cu; however, the difference between Cu and Cu–Ag was very small. This abnormal grain growth combined with the evolution of the uniform cube texture was significant only for Cu–Ag with graphene synthesis. Fig. 1a shows the EBSD result of Cu without Ag, and Fig. 1d shows that of Cu–Ag without graphene; the (100) ratio was low, and the abnormal grain growth did not occur in those samples. Therefore, we have shown that the microstructure of Cu was significantly changed by satisfying both conditions of Cu–Ag alloy formation and graphene synthesis at the same time. If only one condition of alloying with Ag or graphene synthesis on Cu was introduced, the microstructural change of Cu to the cube texture was relatively small. This unusual grain growth of Cu needs not only the condition of graphene synthesis on Cu but also the condition of alloying with Ag.

Fig. 2 shows the evolution of the Cu–Ag microstructure with the extent of graphene synthesis. The Cu texture was compared for the sample before graphene synthesis (point 1 in Fig. 2a) and with graphene synthesis for 10 min (point 2), 20 min (point 3) and 40 min (point 4) at 1000 °C. The temperature profile and EBSD measurement points are shown in Fig. 2a. Fig. 2b shows SEM images of graphene on Cu at synthesis points 2 and 3, and these SEM images show that graphene was progressively synthesized on Cu–Ag (incomplete film) with 10 min and 20 min of synthesis time.

The (100) ratio of Cu increased from point 1 to point 4 according to the degree of graphene synthesis, as shown in the EBSD orientation maps in Fig. 2c. As summarized in Fig. 2d and 2e, grain size abruptly increased with the synthesis of fully grown graphene film, the ratio of the (100) texture was 67.4% for Cu before graphene synthesis, and the ratio increased to 74.2% and 78.9% with 10 min and 20 min of graphene synthesis time, respectively. This value increased to 98.1% after graphene synthesis for 40 min with the formation of the complete graphene film. The ratio of (100) in Cu before graphene synthesis was almost the same as that for the annealed sample shown in Fig. 1d, and this increased with the progress of graphene synthesis. The ratio increased throughout the synthesis time of graphene and finally, most of the Cu orientation was changed to the cube texture with abnormal grain growth of Cu with the complete synthesis of a graphene film. Therefore, the evolution of the (100) texture with abnormal grain growth is related to the progress of the graphene synthesis. The abnormal grain growth of Ag-plated Cu according to the extent of graphene synthesis was clearly demonstrated here, and the Cu texture was changed to the cube texture through graphene synthesis. The effects of graphene synthesis on Cu are critical for the abnormal grain growth of Cu.

To demonstrate the effects of Ag on this unusual microstructural evolution of Cu, the Cu texture was compared in Ni 200 nm plated Cu and Au 200 nm plated Cu. Ni was electroplated using nickel(II) sulfate as the electrolyte, with a deposition rate of 1.13 $\mu m\ min^{-1}$ at 5 ASD and Au was electroplated using potassium gold cyanide as the electrolyte with a deposition rate of 0.12 $\mu m\ min^{-1}$ at 0.3 ASD.

Fig. 3 shows the EBSD orientation maps of Cu–Ni (a) and Cu–Au (b) without graphene and with graphene at 1000 °C for 40 min. The (100) ratio of Cu–Ni was 69.3% without graphene and 58.8% with graphene synthesis and that of Cu–Au was 63.1% without graphene and 57.3% with graphene synthesis. As shown in Fig. 3, abnormal grain growth of Cu was not observed with graphene synthesis on Ni plated Cu and Au plated Cu. From these results, only Ag, not the other plating metals (Ni, Au), affects the microstructural evolution of Cu, and this phenomenon only occurs with graphene synthesis on Cu. We may conclude that the abnormal grain growth of Cu to the cube texture occurs only when both conditions, Cu–Ag alloying and graphene synthesis, are satisfied at the same time.

Why does the abnormal grain growth of Cu occur only for the Ag plated Cu with graphene synthesis? In general, when the stress of Cu exceeds its yield stress, strain relaxation (such as deformation) occurs to reduce the stress. There are two stresses related to this phenomenon; the first is the intrinsic stress due to the Cu–Ag alloy formation, and the other is the interface stress due to the interface formation between Cu and graphene. For Ag plated Cu, intrinsic stress can be induced in Cu by alloy formation with Ag. Ag atoms were diffused in Cu during the ramping-up stage, and then, a substitutional Cu–Ag alloy was formed before graphene synthesis.[11] Ag atoms in substitutional sites of Cu induced the lattice distortion due to the large atomic size of Ag (atomic radii of Ag: 0.144 nm and Cu: 0.128 nm (ref. 17)). Measurement of the actual stress induced by Cu–Ag formation is quite difficult, however, we could estimate which stress is induced by alloy formation from King's concept of volume size factor.[18] A volume size factor, Ω_{sf}, is defined as the effective atomic volume of the solute and Ω_{sf} for Cu–Ag is

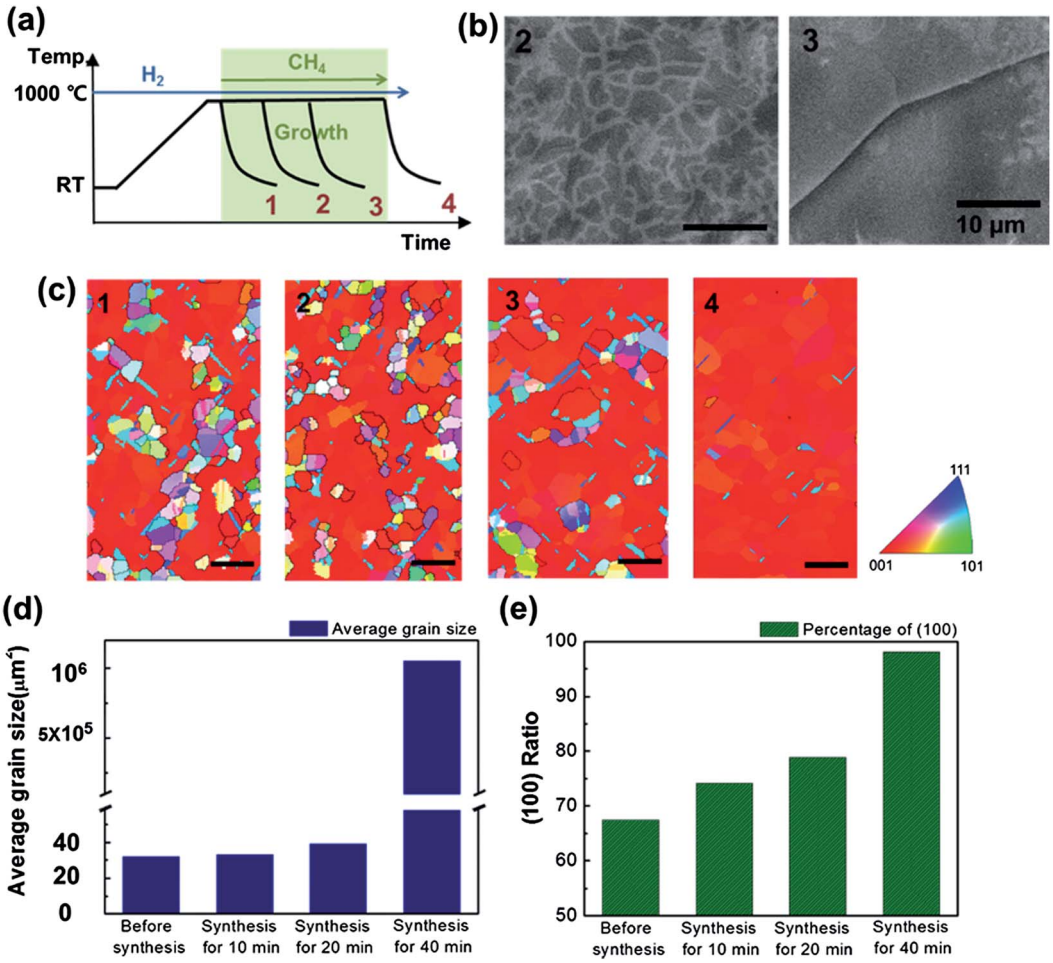

Fig. 2 Evolution of the Cu texture with graphene synthesis progress: (a) the temperature profile of the CVD process, (1) before graphene synthesis after heating up and pre-annealing for 10 min. (2) Graphene synthesis for 10 min. (3) Graphene synthesis for 20 min. (4) Graphene synthesis for 40 min. (b) SEM image of synthesized graphene on Cu–Ag for 10 min (1) and 20 min (2); scale bars (200 μm). (c) EBSD orientation maps of Cu–Ag with graphene synthesis progress through (1–4). (d) The average grain size of Cu and (e) the ratio of the (100) texture with graphene at 1000 °C on Cu–Ag with variation of growth time.

+43.52%. This positive value means that the compressive stress is generated with the Cu–Ag alloy formation.[18,19] In addition, the interface energy on the Cu surface was caused by the binding energy between graphene and Cu. Graphene synthesized on the Cu–Ag alloy was highly uniform[11] and this highly uniform monolayer of graphene on Cu–Ag with van der Waals interactions has a sufficient effect to induce stress on Cu. Graphene is a very strong material (Young's modulus of graphene is about 2 TPa (ref. 20)); graphene could be sustainable for the induced stress. The relative stress of Cu may be smaller than graphene; this stress contributed to the total stress in Cu foil.

The total stress of dilute alloyed Cu after graphene synthesis exceeded the yield stress of Cu; thus, stress relaxation would be induced in the Cu foil. Cu is a face centered cubic (FCC) metal, and the elastic modulus is strongly anisotropic;[17] M_{100} is 115 GPa, M_{110} is 233 GPa and M_{111} is 261 GPa (M_{hkl}: effective biaxial modulus). The strain energy stored in each grain depends on both the grain size and the crystal orientation, and the Cu orientation was changed to the (100) texture for the strain minimization of the Cu foil. If only one of these stresses (*i.e.*, intrinsic stress or interface stress) exists in Cu, the stress is too small to exceed the yield stress of Cu; thus, the Cu texture would not change to the (100) orientation, and abnormal grain growth would not occur. Therefore, the abnormal grain growth of Cu did not occur for Cu–Ag without graphene synthesis (after annealing) or for Cu with graphene synthesis, as discussed above. With regard to the intrinsic stress induced by an alloy metal, Ni has a similar atomic size to that of Cu (atomic radius of Ni: 0.125 nm (ref. 17)), so the lattice distortion due to the substitutional Ni was small for the Cu–Ni alloy. For Cu–Au, although Au has a larger atomic size than Cu (atomic radius of Au: 0.144 nm (ref. 17)), Au atoms were segregated by quenching to room temperature after graphene synthesis due to the miscibility gap between Au and Cu. In addition, Au comprises 0.79% for Cu–Au, so the effect of Au segregation is small. Due to these effects, as discussed above, the abnormal grain growth of Cu occurred only for the Cu–Ag alloy with graphene synthesis.

In other words, the abnormal grain growth of Fe–3% Si and its driving force have been well studied by many researchers.[21,22] Anisotropic energy and solid-state wetting were the main factors

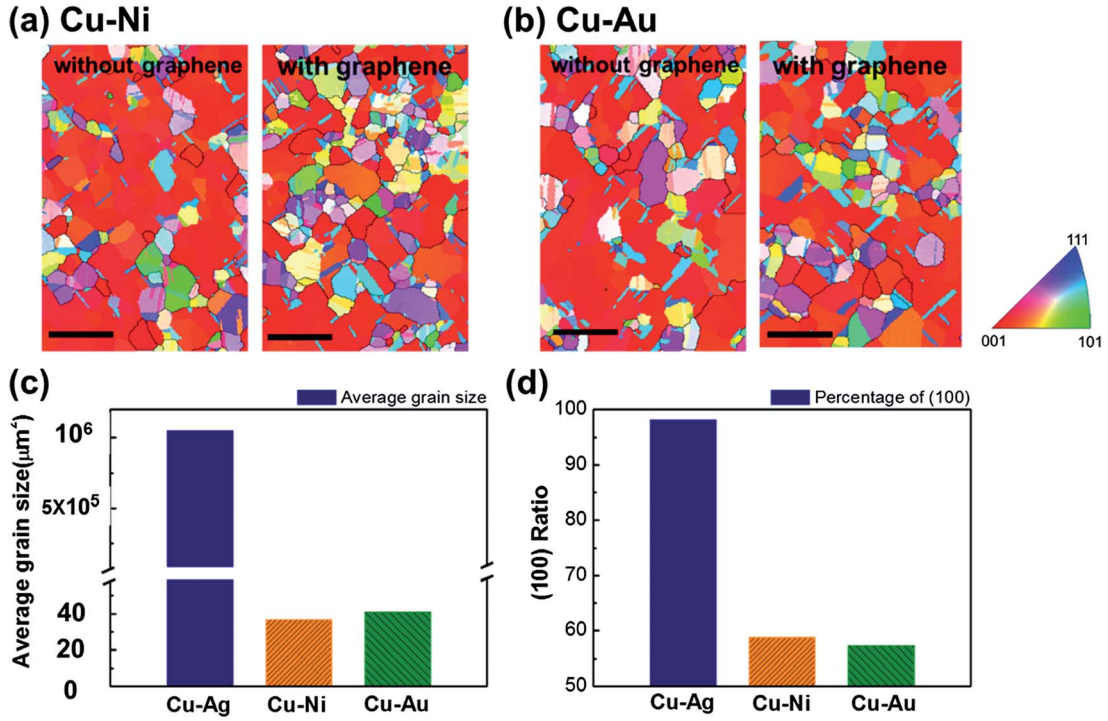

Fig. 3 EBSD orientation maps of Cu–Ni (a) and Cu–Au (b) without graphene and graphene synthesis at 1000 °C for 40 min, scale bars (200 μm). (c) The average grain size of Cu and (d) the ratio of the (100) texture with graphene on Cu–Ag, Cu–Ni and Cu–Au at 1000 °C.

causing the abnormal grain growth of Fe–3% Si; however, the grain growth scale of the Cu–Ag alloy with graphene synthesis was significantly greater than that of Fe–3% Si. Therefore, the angstrom-scale thickness of graphene, with one atomic layer, has a remarkable effect on the microstructural evolution of Cu with abnormal grain growth. Graphene has only one atomic layer with a 3.45 Å thickness, which is far thinner than the 35 μm thick Cu foil. However, a monolayer of graphene induced large stress in Cu, and this phenomenon of 18 750 times larger grain growth of Cu was very unusual.

If the Cu has a preferred orientation over the entire area of Cu foil, homogeneous electrical and mechanical characteristics of Cu could be obtained despite the anisotropic properties of Cu. The electrical conductivity and ductility would be higher than those of polycrystalline Cu due to the large grains with (100)⟨100⟩ cube texture. This could be beneficial for various applications of Cu with overall cube texture.

Conclusions

We investigated the abnormal grain growth of Cu with graphene synthesis and Cu–Ag alloy formation. The Cu formed giant grains with (100)⟨100⟩ cube texture and with sizes greater than 1.05 mm^2. The abnormal grain growth occurred only for the Cu–Ag alloy substrate with graphene synthesis, and this grain growth did not occur if only one of these conditions (Ag or graphene) was present. This phenomenon was caused by the intrinsic stress from Cu–Ag alloy formation and the interface energy between Cu and graphene with graphene synthesis.

Acknowledgements

This work was supported by the Global Leading Technology Program of the Office of Strategic R&D Planning (OSP) funded by the Korean government (Ministry of Trade, Industry & Energy) (No. 10042537) and the Global Frontier Research Program (2011-0031627).

Notes and references

1 K. S. Novoselov, A. K. Geim, S. V. Morozov, D. Jiang, Y. Zhang, S. V. Dubonos, I. V. Grigorieva and A. A. Firsov, *Science*, 2004, **306**, 666–669.
2 Y. Zhang, Y.-W. Tan, H. L. Stormer and P. Kim, *Nature*, 2005, **438**, 201–204.
3 A. K. Geim and K. S. Novoselov, The rise of graphene, *Nat. Mater.*, 2007, **6**, 183–191.
4 I. W. L. Frank, D. M. Tanenbaum, A. M. Van der Zande and P. L. McEuen, *J. Vac. Sci. Technol., B: Microelectron. Nanometer Struct.–Process., Meas., Phenom.*, 2007, **25**, 2558–2561.
5 A. A. Balandin, S. Ghosh, W. Z. Bao, I. Calizo, D. Teweldebrhan, F. Miao and C. N. Lau, *Nano Lett.*, 2008, **8**, 902–907.
6 R. R. Nair, P. Blake, A. N. Grigorenko, K. S. Novoselov, T. J. Booth, T. Stauber, N. M. R. Peres and A. K. Geim, *Science*, 2008, **320**, 1308.
7 Q. Yu, L. A. Jauregui, W. Wu, R. Colby, J. Tian, Z. Su, H. Cao, Z. Liu, D. Pandey, D. Wei, T. F. Chung, P. Peng,

N. P. Guisinger, E. A. Stach, J. Bao, S.-S. Pei and Y. P. Chen, *Nat. Mater.*, 2011, **10**, 443–449.
8 G. H. Han, F. Gunes, J. J. Bae, E. S. Kim, S. J. Chae, H.-J. Shin, J.-Y. Choi, D. Pribat and Y. H. Lee, *Nano Lett.*, 2011, **11**(10), 4144–4148.
9 J. D. Wood, S. W. Schmucker, A. S. Lyons, E. Pop and J. W. Lyding, *Nano Lett.*, 2011, **11**(11), 4547–4554.
10 J. Tian, H. Cao, W. Wu, Q. Yu, N. P. Guisinger and Y. P. Chen, *Nano Lett.*, 2012, **12**(8), 3893–3899.
11 H.-A.-S. Shin, J. Ryu, S.-P. Cho, E.-K. Lee, S. Cho, C. Lee, Y.-C. Joo and B. H. Hong, *Phys. Chem. Chem. Phys.*, 2014, **16**, 3087–3094.
12 S. Suwas and N. P. Gurao, *J. Indian Inst. Sci.*, 2008, **88**(2), 152–177.
13 T. Kamijo, A. Fujiwara, Y. Yoneda and H. Fukutomi, *Acta Metall. Mater.*, 1991, **39**, 1947–1952.
14 J. Greiser, D. Muller, P. Mullner, C. V. Thompson and E. Arzt, *Scr. Mater.*, 1999, **41**(7), 709–714.
15 J. Greiser, P. Mullner and E. Arzt, *Acta Mater.*, 2001, **49**, 1041–1050.
16 C. V. Thompson, *Annu. Rev. Mater. Sci.*, 2000, **30**, 159.
17 *Materials science and engineering: an introduction*, ed. W. D. Callister, 7th edn, 2007.
18 H. W. King, *J. Mater. Sci.*, 1966, **1**, 79.
19 M. S. Yoon, M. K. Ko, O. H. Kim, Y. B. Park, W. D. Nix and Y. C. Joo, *J. Electron. Mater.*, 2007, **36**, 562.
20 J.-U. Lee, D. Yoon and H. Cheong, *Nano Lett.*, 2012, **12**, 4444–4448.
21 N. M. Hwang, *J. Mater. Sci.*, 1998, **33**, 5625–5629.
22 H. Park, D.-Y. Kim, N.-M. Hwang, Y.-C. Joo, C. H. Han and J.-K. Kim, *J. Appl. Phys.*, 2004, **95**(10), 5515–5521.